This article is published as part of the *Dalton Transactions* themed issue entitled:

Dalton Transactions 40th Anniversary

Guest Editor Professor Chris Orvig, Editorial Board Chair
University of British Columbia, Canada

Published in issue 40, 2011 of *Dalton Transactions*

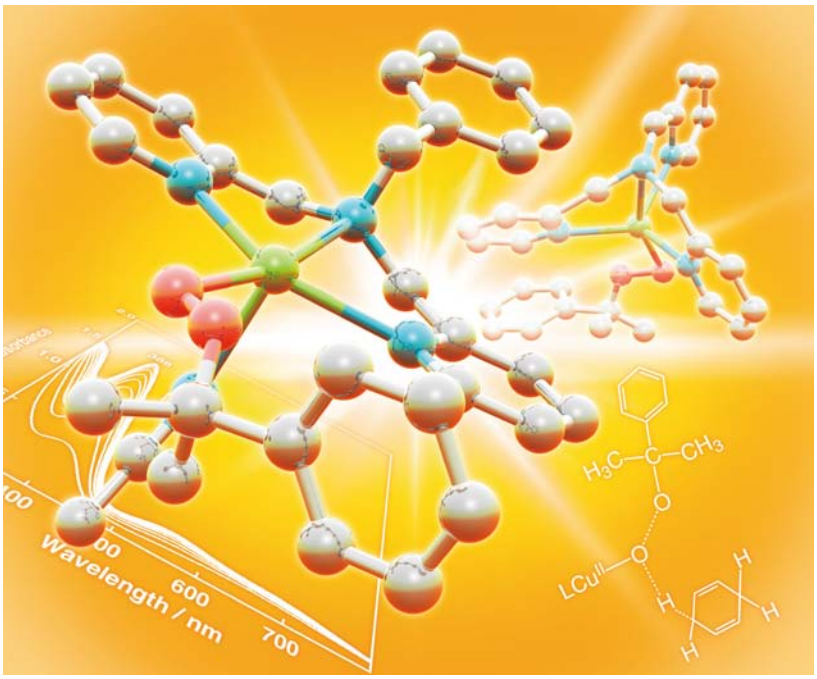

Image reproduced with permission of Shinobu Itoh

Welcome to issue 40 of the 40th volume of Dalton Transactions-40/40! Articles in the issue include:

PERSPECTIVE:

Synthesis and coordination chemistry of macrocyclic ligands featuring NHC donor groups
Peter G. Edwards and F. Ekkehardt Hahn
Dalton Trans., 2011, 10.1039/C1DT10864F

FRONTIER:

The future of metal–organic frameworks
Neil R. Champness
Dalton Trans., 2011, DOI: 10.1039/C1DT11184A

ARTICLES:

Redox reactivity of photogenerated osmium(II) complexes
Jillian L. Dempsey, Jay R. Winkler and Harry B. Gray
Dalton Trans., 2011, DOI: 10.1039/C1DT11138H

Molecular squares, cubes and chains from self-assembly of bis-bidentate bridging ligands with transition metal dications
Andrew Stephenson and Michael D. Ward
Dalton Trans., 2011, DOI: 10.1039/C1DT10263J

Visit the *Dalton Transactions* website for more cutting-edge inorganic and organometallic research
www.rsc.org/dalton

Dalton Transactions

Dynamic Article Links

Cite this: *Dalton Trans.*, 2011, **40**, 10526

www.rsc.org/dalton

PAPER

Synthesis, characterization, and single-molecule metamagnetism of new Co(II) polynuclear complexes of pyridine-2-ylmethanol†

Roberto Pattacini,[a] Peili Teo,[a,b] Jun Zhang,[a,b] Yanhua Lan,[c] Annie K. Powell,[c] Joscha Nehrkorn,[d] Oliver Waldmann,[d] T. S. Andy Hor[b] and Pierre Braunstein[a]

Received 12th April 2011, Accepted 5th July 2011
DOI: 10.1039/c1dt10631g

The reaction between pyridine-2-ylmethanol (HL), anhydrous $CoCl_2$ and NaH afforded polynuclear Co(II) complexes $[Co_7(L)_{12}]Cl_2$ (**1**), $[Co_6Na(L)_{12}]Cl$ (**2**) and $[Co_4Cl_2(L)_6]$ (**3**), depending on the HL:$CoCl_2$ ratio set in the reaction. The core structures of the centrosymmetric complexes **1** and **2** are of the M@Co_6 type (M = Co or Na, respectively) with a coplanar arrangement of the metals whereas that of centrosymmetric **3** is of an incomplete dicubane type. The experimental conditions allowing interconversions between these polynuclear complexes have been determined, which provides a more rational control of their synthesis. Thus, **1** transforms to **3** when reacted with $CoCl_2$ in a 1 : 1 ratio, whereas the same reaction performed with a large excess of $CoCl_2$ gave the tetranuclear pseudo-cubane complex $[Co_4(L)_4Cl_2(MeOH)_4]$ upon recrystallization. Conversely, **1** was isolated from the reaction of **3** with HL and NaH. The crystal structure of these compounds is reported, along with the magnetic behaviour of **1** and **3**. The analysis of the magnetism using the effective spin-1/2 Hamiltonian approach revealed single-molecule metamagnetic behavior in **3**.

Introduction

Pyridyl-alcoholates can be efficiently used as ligands for the formation of polynuclear complexes. In particular, pyridin-2-ols (or their tautomers 2-pyridinones)[1] and pyridine-2-ylmethanol[2] (HL, Scheme 1) proved to be convenient commercial precursors for the synthesis of such compounds, owing to their N,O chelation capabilities, their relatively high acidity and, when deprotonated, the efficient O-bridging coordination over two or three metal centres (Scheme 1).

However, despite the rich chemistry of pyridine-2-ylmethanolate (L^-), novel high nuclearity Ni(II) complexes could be recently isolated from relatively simple reactions. Thus, reactions between HL, $[NiCl_2(DME)]$ (DME = dimethoxyethane) and NaH afforded the polynuclear complexes $[Ni_7(L)_{12}]Cl_2$, $[NaNi_6(L)_{12}]Cl$, $[Na_3Ni_4(L_9)(\mu_3\text{-}OH)]Cl$ and $[Na_{10}Ni_6(L)_{20}(\mu_5\text{-}OH)_2]$,which are characterized by a L/Ni ratio of 1.71, 2, 2.25 and 3.3, respectively.[3] Despite the complexity of the system due to the diversity of products formed, some synthetic control could be achieved by varying the initial HL/Ni ratio in a manner that parallels the L/Ni ratio observed in the product.

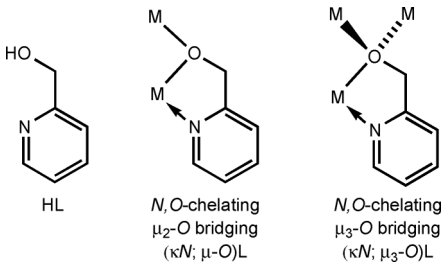

Scheme 1 Ligand HL and its bonding modes in polynuclear complexes.

The anionic ligand L^- has also been used for the preparation of the structurally characterized Co(II) tetranuclear pseudo-cubane complex $[Co(L)Cl(MeOH)]_4$ (Scheme 2).[4] This complex was obtained by reaction of NaOMe with $CoCl_2$ and HL in methanol, but synthetic details and spectroscopic characterization were not provided. It was the first member of the fast-growing family of cobalt Single Molecule Magnets (SMM).[5]

Such cobalt-based SMMs remain however relatively few, when compared to the families of Mn- and Fe-containing SMMs.[6] Furthermore, the interpretation of the magnetism in Co(II) coordination clusters is notoriously difficult because of the unquenched orbital angular momentum of high-spin Co(II).[7] However, exactly

[a]*Laboratoire de Chimie de Coordination, UMR 7177 CNRS/Université de Strasbourg, Institut Le Bel 4, Rue Blaise Pascal, CS90032, 67081, Strasbourg Cedex, France. E-mail: braunstein@unistra.fr; Fax: +33 368851322; Tel: +33 368851308*

[b]*Department of Chemistry, National University of Singapore, 3, Science Drive 3, Singapore, 117543, Singapore*

[c]*Institute of Inorganic Chemistry, Karlsruhe Institute of Technology (KIT), Engesserstrasse 15, 76131, Karlsruhe, Germany*

[d]*Physikalisches Institut, Universität Freiburg, Hermann-Herder-Strasse 3, 79104, Freiburg, Germany*

† Electronic supplementary information (ESI) available: FTIR spectra of compounds **1**–**3**, mass spectra of $[Co_6Mg(L_{12})]^{2+}$ and $[CaCo_6(L_{12})]^{2+}$, details of the X-ray refinement, additional susceptibility plot of **3** and ac susceptibility data for **1** and **3**. CCDC reference numbers 821779–821781. For ESI and crystallographic data in CIF or other electronic format see DOI: 10.1039/c1dt10631g

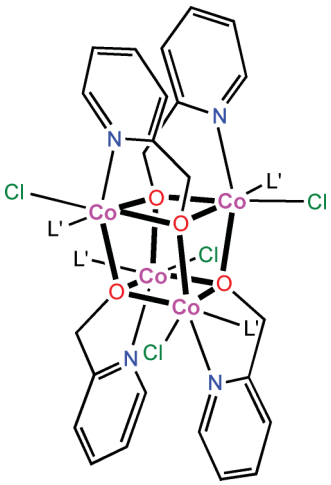

Scheme 2 [Co(L)Cl(MeOH)]$_4$, L′ = MeOH.[4]

this property can give rise to magnetic properties not usually observed in other types of coordination clusters, for instance the rarely observed metamagnetic-like behaviour in a single molecule.[8]

Thus, by analogy with the observations made in the Ni(II) chemistry, we wondered if the fine-tuning of the reaction conditions could give rise to the isolation of possibly overlooked Co(II) complexes of higher nuclearity. In addition, we shall see that, differently from most previous cases where Co(II) polynuclear complexes have been isolated, we were able to achieve some synthetic control and explore interconversion reactions linking the different types of structures encountered.

Indeed, a rationalization of the experimental conditions under which a given polynuclear complex is obtained is highly desirable since in most cases isolation occurs, in variable yields, by crystallization from complex reaction mixtures. As recently stated, "*in order to be able to control the magnetic properties of SMMs, we need control over many aspects of the composition and structure of polynuclear complexes. The fact that these complexes are often synthesised and crystallised straight from a one-pot reaction, in one step, means that often we have little synthetic control. This is especially important when using a multidentate ligand, with many binding sites and many different binding modes.*"[6]

Results and discussion

Synthesis

The reaction between pyridine-2-ylmethanol (HL) (1.8 equiv.), anhydrous $CoCl_2$ (1 equiv.) and NaH (2.5 equiv.) was performed in THF. It afforded the polynuclear complexes $[Co_7(L)_{12}]Cl_2$ (**1**), $[Co_6Na(L)_{12}]Cl$ (**2**) and $[Co_4Cl_2(L)_6]$ (**3**) in 38%, 5% and 35% yield, respectively (Scheme 3).

Compounds **1** and **3** are poorly soluble in THF and they were easily collected by filtration at the end of the reaction. They were then dissolved in CH_2Cl_2 and layering of these solutions with Et_2O gave a mixture of orange and violet crystals of **1** and **3**, respectively. Taking advantage of the dissolution inertia of the crystals of **3** in CH_2Cl_2, it was possible to separate this complex from **1**, whose crystals, in contrast, quickly dissolve in this solvent. Compound **2** is the only soluble species in THF and it was obtained in low yield

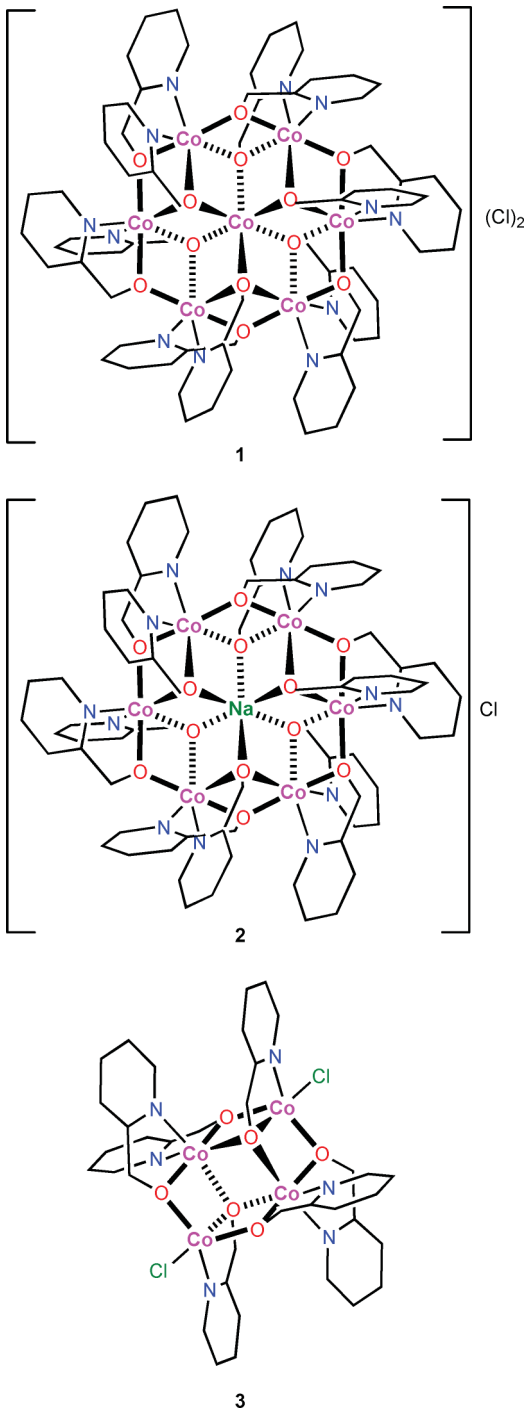

Scheme 3 Structures of complexes **1**–**3**. Aromatic bonds in pyridine rings omitted for clarity.

by crystallization from the reaction mixture after filtration. Eqn (1)–(3) account for the formation of the products.

$$7\ CoCl_2 + 12\ HL + 12\ NaH \rightarrow 12\ H_2\uparrow + [Co_7(L)_{12}]Cl_2\ (\mathbf{1})\downarrow + 12\ NaCl\downarrow \quad (1)$$

$$6\ CoCl_2 + 12\ HL + 12\ NaH \rightarrow 12\ H_2\uparrow + [Co_6Na(L)_{12}]Cl\ (\mathbf{2}) + 11\ NaCl\downarrow \quad (2)$$

$$4\ CoCl_2 + 6\ HL + 6\ NaH \rightarrow 6\ H_2\uparrow + [Co_4(L)_6Cl_2]\ (\mathbf{3})\downarrow + 6\ NaCl\downarrow \quad (3)$$

More convenient and higher yield syntheses of **1** and **3** were achieved when 2.2 or 1.6 equivalents of HL, respectively, were reacted with $CoCl_2$ in the presence of an excess of NaH. Cluster **1** could be isolated in good yields with HL:$CoCl_2$ ratios between 2 and 3, whereas with any ratio between 1.6 and 2, both **1** and **3** were obtained. Formation of **3** requires that HL should be added to a freshly prepared suspension of $CoCl_2$ in THF and not to a solution of $CoCl_2$. Indeed, complete solubilisation of $CoCl_2$ prior to the addition of HL leads to no reaction with NaH. This is due to the rapid formation of inert Co(II) complexes of HL, not prone to deprotonation. The presence of NaL in solution, which can be prepared *in situ* by reaction of NaH with HL, is required for the formation of **1–3**. Depending on the HL:$CoCl_2$ ratio, **1** or **3** are instantly formed upon addition of $CoCl_2$ to a solution of NaL.

These observations are consistent with those made in the related Ni(II) system.[3b]

In the early stages of the reaction giving **1**, the colour of the suspension became violet, before turning to orange yellow. This suggested that cluster **3** could be an intermediate in the formation of **1**. Indeed, **1** could be isolated from the 1 : 1 : 1 reaction of pure **3** with HL and NaH (eqn (4)):

$$7\,[Co_4(L)_6Cl_2]\,(\mathbf{3}) + 6\,HL + 6\,NaH \rightarrow 3\,H_2\uparrow + 4\,[Co_7(L)_{12}]Cl_2\,(\mathbf{1})\downarrow + 6\,NaCl\downarrow \quad (4)$$

Conversely, complex **3** was isolated from the reaction of **1** with a stoichiometric amount of $CoCl_2$ (eqn (5)). This reaction is slow in THF, most likely because of the poor solubility of **1** in this solvent, whereas in CH_2Cl_2 complete conversion was achieved in one hour.

$$[Co_7(L)_{12}Cl_2]\,(\mathbf{1}) + CoCl_2 \rightarrow 2\,[Co_4(L)_6Cl_2]\,(\mathbf{3}) \quad (5)$$

When the latter reaction was performed with a large excess of $CoCl_2$, rapid formation of **3** was observed by FTIR spectroscopy. However, complex **3** was then rapidly consumed with formation of a new product, showing an FTIR pattern consistent with a cubane-like complex of the type $[Co(L)Cl]_4$, possibly solvated (see ESI†). Indeed, $[Co(L)Cl(MeOH)]_4$ (Scheme 2) was isolated by recrystallization of this unknown product from methanol. Eqn (6) accounts for the formation of $[Co_4(L)_4Cl_2(MeOH)_4]$ from **3**.

$$2\,[Co_4(L)_6Cl_2]\,(\mathbf{3}) + 4\,CoCl_2 + 4\,MeOH \rightarrow 3\,[Co_4(L)_4Cl_2(MeOH)_4] \quad (6)$$

The X-ray molecular structures of **1**, **2** and **3** were determined by single crystal X-ray diffraction and are reported below.‡In the centrosymmetric, heptanuclear structure of the cation $[Co_7(L)_{12}]^{2+}$ (Fig. 1), six of the seven metal centres (Co2, Co3, Co4 and their centrosymmetric equivalents Co2′, Co3′, Co4′) form a slightly distorted hexagon, while the seventh Co atom is disposed at its centroid. Each of the peripheral metals is bischelated by two L monoanions, through the N and O atoms. Each edge of the distorted hexagon is doubly bridged by alcoholate functions, one of which further coordinates the central metal, thus acting as a μ_3-capping ligand. The Co–(μ_2-O)–Co angles [spanning from 103.2(2) to 103.9(2)°] are wider than the Co–(μ_3-O)–Co ones [94.4(1)–99.4(2)°]. The μ_3-O bridges are not symmetrical. Thus, for example, the Co1–O1, Co2–O1 and Co3–O1 distances are 2.100(5), 2.061(3) and 2.208(4) Å, respectively. The shorter

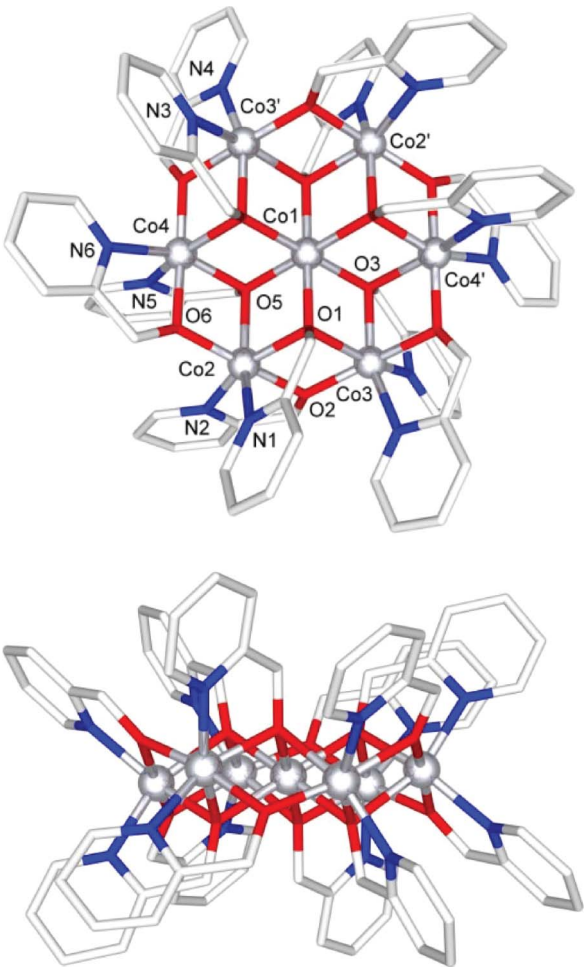

Fig. 1 Diagrams of the molecular structure of the $[Co_7(L)_{12}]^{2+}$ cation in **1**·4CH_2Cl_2. Selected distances (Å) and angles (deg): Selected distances and angles: Co1–Co2 3.1726(9), Co1–Co3 3.173(1), Co1–Co4 3.1615(7), Co2–Co3 3.183(1), Co2–Co4 3.174(2), Co3–Co4′ 3.184(1); Co1–O1–Co2 99.4(2), Co1–O5–Co2 94.4(1), Co1–O1–Co3 94.8(2), Co1–O3–Co3 98.7(2), Co1–O5–Co4 97.8(2), Co1–O3′–Co4 94.3(1), Co2–O2–Co3 103.2(2), Co2–O6–Co4 103.2(2), Co3–O3–Co4′ 95.8(2), Co3–O4–Co4′ 103.9(2). Symmetry operations generating equivalent atoms (′): -x, -y, -z.

‡ Crystal data for **1**: $C_{72}H_{72}Co_7N_{12}O_{12}\cdot 4(CH_2Cl_2)\cdot 2(Cl)$, M = 2120.53, triclinic, a = 12.495(7) Å, b = 14.180(1) Å, c = 14.571(1) Å, α = 61.785(3)°, β = 73.167(4)°, γ = 75.014(4)°, V = 2154.7(12) Å^3, T = 173(2)K, space group $P\bar{1}$, Z = 1, μ = 1.689 mm^{-1}, 12470 reflections measured, 9116 independent reflections (R_{int} = 0.0510). The final R_1 values were 0.0622 ($I > 2\sigma(I)$). The final $wR(F^2)$ values were 0.1105 ($I > 2\sigma(I)$). The final R_1 values were 0.2014 (all data). The final $wR(F^2)$ values were 0.1341 (all data). The goodness of fit on F^2 was 0.985.Crystal data for **2**: $C_{72}H_{72}ClCo_6N_{12}NaO_{12}\cdot 2CH_2Cl_2$, M = 1879.29, triclinic, a = 10.2761(7) Å, b = 13.5914(9) Å, c = 14.2153(9) Å, α = 93.0970(10)°, β = 95.1830(10)°, γ = 90.9820(10)°, V = 1973.9(2) Å^3, T = 293(2)K, space group $P\bar{1}$, Z = 1, μ = 1.474 mm^{-1}, 21040 reflections measured, 9021 independent reflections (R_{int} = 0.0272). The final R_1 values were 0.0483 ($I > 2\sigma(I)$). The final $wR(F^2)$ values were 0.1375 ($I > 2\sigma(I)$). The final R_1 values were 0.0566 (all data). The final $wR(F^2)$ values were 0.1432 (all data). The goodness of fit on F^2 was 1.078.Crystal data for **3**: $C_{36}H_{36}Cl_2Co_4N_6O_6\cdot CH_2Cl_2$, M = 1040.25, triclinic, a = 9.5440(8) Å, b = 10.7320(9) Å, c = 11.2030(8) Å, α = 89.128(4)°, β = 65.639(4)°, γ = 76.750(4)°, V = 1013.41(14) Å^3, T = 173(2)K, space group $P\bar{1}$, Z = 1, μ = 1.926 mm^{-1}, 6414 reflections measured, 4390 independent reflections (R_{int} = 0.0286). The final R_1 values were 0.0419 ($I > 2\sigma(I)$). The final $wR(F^2)$ values were 0.0895 ($I > 2\sigma(I)$). The final R_1 values were 0.0696 (all data). The final $wR(F^2)$ values were 0.0985 (all data). The goodness of fit on F^2 was 1.061.

distance corresponds to the Co–O bond participating in the chelation ring. Similar observations apply to the remaining μ_3-O systems.

Overall, the cation displays a non-crystallographic S_6 (C_{3i}) symmetry, and can be described as possessing a M@M_6 Anderson-type structure, with a CdI_2-type (or brucite) arrangement for the Co_7O_{12} core. Two chlorides act as counterions, relatively far away from the metals. As expected, the structure shares close similarities with that of the related complex $[Ni_7(L)_{12}]^{2+}$.[3b] When compared to the latter cation, **1** displays a slightly expanded core, with Co1–Co distances [ranging from 3.1615(7) to 3.173(1) Å] longer than those between the central Ni atom and the outer ones in $[Ni_7(L)_{12}]^{2+}$ [from 3.1196(7) to 3.1230(7) Å]. The distances involving neighbouring atoms of the hexagon show a similar trend (from 3.174(2) to 3.184(1) Å in **1**, from 3.1250(9) to 3.1415(8) Å in $[Ni_7(L)_{12}]^{2+}$). This complies well with the differences in ionic radii of the respective metal cations [0.69 and 0.74 Å for Ni(II) and high spin Co(II), respectively].[9]

The Co@Co_6 topology observed in **1** has been previously observed in cobalt complexes with μ_3-*O*-bridging ligands. The examples reported in the literature deal with Co(II)/Co(III) mixed-valence species,[10] or $Co(II)_7$ complexes of the type of **1**, and $[Co_7(mmap)_5(\mu_3\text{-}X)][ClO_4]_2$ (mmap = 2-methoxy-6-[(methylimino)-methyl]phenolate, X = OH, CH_3O or N_3).[11] Azido-bridged $Co(II)_7$ coordination clusters have also been reported.[12]

The structure of the monocation $[Co_6Na(L)_{12}]^+$ in **2** (Fig. 2) is similar to that of **1**, but with a sodium cation replacing the central cobalt ion. The larger radius of Na^+ (1.66 Å) with respect to that of high spin Co(II) (1.50 Å)[13] results in longer O–Na distances (ranging from 2.273(2) to 2.287(2) Å), with respect to the O–Co1 ones in **1** (from 2.100(5) to 2.135(3) Å). However, the M···M separations in **2** are similar to those in **1**, with Na···Co distances (ranging from 3.1248(4) to 3.1933(5) Å) comparable to the Co1···Co distances in **1**. The Co···Co separations between neighbouring atoms forming the outer hexagon (ranging from 3.1612(4) to 3.1817(6) Å) are as well analogous to those in **1**. The structural changes needed to accommodate the larger Na^+ cation are achieved by the slight narrowing of the Na–O–Co angles (mean value 91.57(8)°) with respect to the Co–O–Co1 angles in **1** (mean value 96.6(2)°).

Although Na@M_6 (M = transition metal) structures have been reported,[14] this was not the case in cobalt chemistry, to the best of our knowledge. However, Co(II)-sodium polynuclear compounds featuring N,O bridging ligands have been reported.[1c,1f,15]

The neutral cluster **3** (Fig. 3) adopts a tetranuclear, centrosymmetric structure of an incomplete dicubane type. Two Co atoms (Co2 and Co2′) show distorted octahedral environments and are bis-chelated by two L anions, with the N and O donors in mutual *cis* and *trans* position, respectively. The alcoholate functions further act as μ_2-bridges, connecting Co2 (and its centrosymmetric counterpart) to Co1′ and Co1. Each of the latter two metal centres is coordinated by a terminal chloride and chelated by a L ligand, whose oxygen is further coordinated to Co2 and Co2′ in a μ_3-capping manner. The coordination geometry around Co1 and Co1′ can be described as trigonal bipyramidal. The tetranuclear structure of **3** is thus different from that of a $Co_4(\mu_3\text{-}O)_4$ cubane of the type depicted in Scheme 2. Considering the metal atoms and the μ_3 oxygen atoms of **3**, two incomplete Co_3O_4 cubane subunits sharing a Co_2O_2 face can be identified. The structure of **3** shares similarities with that of $[Co_4Cl_2(OC_2H_4OEt)_6]$ (OC_2H_4OEt = 2-ethoxy-ethanol),[16] which features an O,O-chelating/bridging ligand, and of $[Co_4(hqd_{-H})_6\ Cl_2]$ (hqd = 8-hydroxyquinaldine).[17] The tetranuclear THF solvate of $CoCl_2$, namely $[Co_4(\mu_3\text{-}Cl)_2(\mu_2\text{-}Cl)_4Cl_2(THF)_6]$[18] displays a related ligand arrangement, with

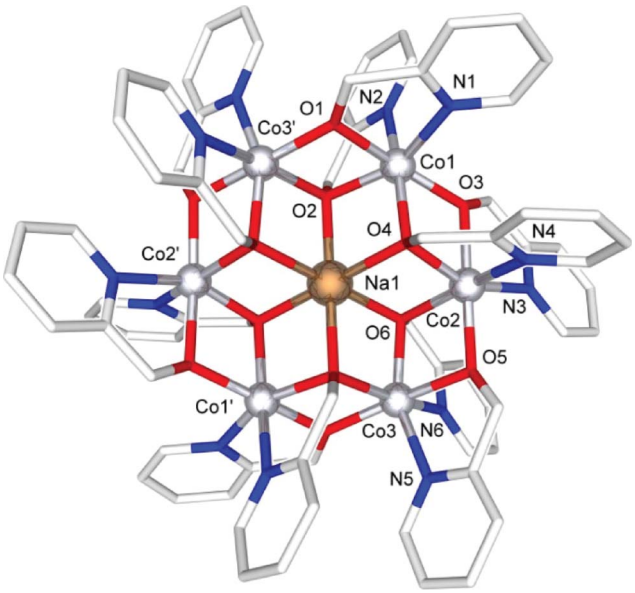

Fig. 2 Diagram of the molecular structure of the $[Co_6Na(L)_{12}]^+$ cation in **2**·$2CH_2Cl_2$. Selected distances (Å) and angles (deg): Co1–Co2 3.1541(6), Co1–Co3′ 3.1669(6), Co2–Co3 3.1817(6), Co1–Na1 3.1612(4), Co2–Na1 3.1933(5), Co3–Na1 3.1248(4); Co1–O1–Co3′ 101.62(9), Co1–O2–Co3′ 97.84(9), Co1–O2–Na1 93.58(8), Co3′–O2–Na1 90.11(8), Co1–O4–Na1 90.60(7), Co1–O4–Co2 97.52(8), Co2–O4–Na1 95.42(8), Co2–O6–Na1 91.18(8), Co2–O5–Co3 102.6(1), Co2–O6–Co3 97.46(9), Co3–O6–Na1 92.02(8). Symmetry operations generating equivalent atoms (′): -x, -y, -z.

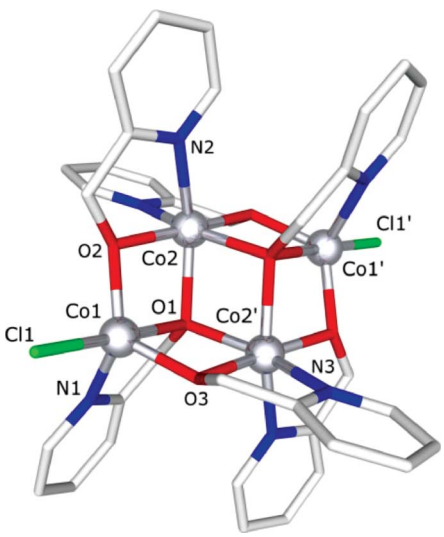

Fig. 3 Diagram of the molecular structure of **3** in **3**·CH_2Cl_2. Selected distances (Å) and angles (deg): Selected distances and angles: Co1···Co2′ 3.1440(6), Co1···Co2 3.1582(7); Co1–O2–Co2 104.47(9), Co1–O1–Co2 92.59(8), Co1–O1–Co2′ 91.97(8), Co1–O3–Co2′ 104.0(1), Co2–O1–Co2′ 101.42(9). Symmetry operations generating equivalent atoms (′): -x, -y, -z.

bridging chlorides ligands instead of the alcoholate bridges in **3**.

In view of the presence of the Na^+ cation in **2**, at the position occupied by the central Co(II) ion in **1**, we attempted to insert other metal cations in this position. Thus, in preliminary experiments, examination of the mass spectra of the reaction mixture containing NaL, $CoCl_2$ and $MgCl_2$ in a 2.5 : 1 : 0.17 ratio, revealed a peak at m/z 837, consistent with the presence of the dication $[Co_6Mg(L)_{12}]^{2+}$. A second, slightly less intense peak was observed at m/z = 854, which corresponds to $[Co_7(L)_{12}]^{2+}$. When the same experiment was carried out using $CaCl_2$ instead of $MgCl_2$, the mass spectrum contained a peak at m/z 845, consistent with the formation of $[Co_6Ca(L)_{12}]^{2+}$ (see ESI†).

Although the Ni(II) analogues of **1** and **2** have been isolated from the corresponding reaction, an interesting difference between the Co(II) and Ni(II) systems lies in the isolation of complex **3**, in which two of the metal centres are in a trigonal bipyramidal environment, whereas in the aforementioned Ni(II) polynuclear complexes, all nickel ions featured octahedral coordination.

Magnetic properties

Magnetic studies were carried out on polycrystalline samples of **1** and **3** dispersed in Apiezon grease, in the temperature range from 1.8 to 300 K. The temperature dependence of the dc magnetic susceptibility and the field dependence of magnetization at different temperatures are displayed in Fig. 4 and 5. The ac susceptibility of compounds **1** and **3** in zero dc field shows a complete absence of out-of-phase components above 1.8 K (Fig. S12–S13†) indicating that no slow relaxation is observed and both compounds are not SMMs.

For **1** the room temperature χT value of 19.09 cm^3 K mol^{-1} is higher than the spin-only value of seven high-spin Co(II) ions [13.125 cm^3 K mol^{-1}, $(\chi T)_{RT} = n\{g^2S(S+1)\}/8$; $S = 3/2$, $n = 7$, $g \sim 2$]. The measured χT value corresponds to $g \sim 2.41$, which is a typical finding for coordination clusters (*i.e.* complexes with well-defined aggregation of coordinatively linked metal ions, usually showing cooperative properties) containing Co(II) ions,[7,8] and reflects the effects of spin-orbit coupling in the compound. The χT value decreases on lowering the temperature, indicating an overall antiferromagnetic coupling between the Co(II) ions. The low-temperature field dependence of the magnetization for compound **1** (Fig. 4, lower panel) shows that the magnetization increases steadily to reach 14.3 μ_B at 2 K and 7 T, which is consistent with a system consisting of seven high-spin Co(II) ions ($7 \times 2.04\ \mu_B$).[7,8]

For compound **3**, the experimental room temperature χT value of 10.20 cm^3 K mol^{-1} (Fig. 5) is higher than the spin-only value of 7.48 cm^3 K mol^{-1} [$S = 3/2$, $n = 4$, $g \sim 2$]. The derived g of 2.33 is smaller than for **1** since **3** also contains two trigonal bipyramidal Co(II) centres, for which the spin-orbit coupling is effective only in second order, *i.e.*, the orbital angular momentum is quenched. Upon lowering the temperature, the χT product continuously decreases and finally reaches 0.47 cm^3 K mol^{-1} at 1.8 K, indicating the presence of antiferromagnetic interactions amongst the paramagnetic centres. A maximum in the χ *vs.* T plot (Figure S-11) observed at 10 K further supports the presence

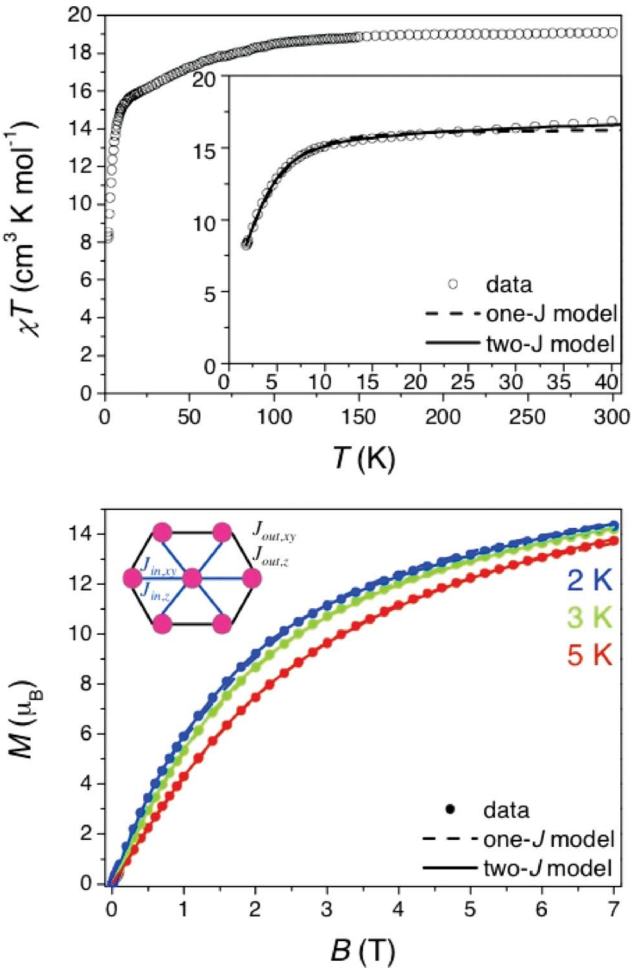

Fig. 4 Plots of χT *vs.* T under applied dc field of 0.1 T (upper) and M *vs.* B curves at the indicated temperatures (lower) for **1**. Data are represented by circles. Dashed lines are fits with the simple model and solid lines are fits with the realistic model (see text). Inset to upper panel: χT *vs.* T in the temperature range used in the fitting. Inset to lower panel: Sketch of the assumed coupling scheme.

of significant antiferromagnetic interactions. The magnetization behaviour is somewhat unusual for a Co(II) cluster in that the magnetization curves at 2, 3 and 5 K increase with an S-shape, with a crossing at around 3.8 T, finally approaching 6.8 μ_B at 7 T but without saturation (Fig. 4, inset). The S-shape and crossing of the M *vs.* B curves can also be seen in plots of dM/dB *vs* B (Fig. 5, right inset), where the maxima correspond to a characteristic field. This behaviour is typically seen when the magnetic field overcomes antiferromagnetic interactions, abruptly changing the magnetic ground state of the system.

The dc magnetic data of **1** and **3** were analyzed by least-square fitting methods, using the effective spin-1/2 formalism for the Co(II) coordination clusters. In an uncoupled high-spin Co(II) ion, the combined effect of distorted octahedral ligand field and spin-orbit coupling produces six Kramer's doublets with energy splitting on the order of 100 K. Thus, at low temperatures (below *ca.* 40 K), where only the ground-state Kramer's doublet is thermally populated, each Co(II) ion can be described by an effective spin 1/2.[19] The Zeeman term for a Co(II) ion then

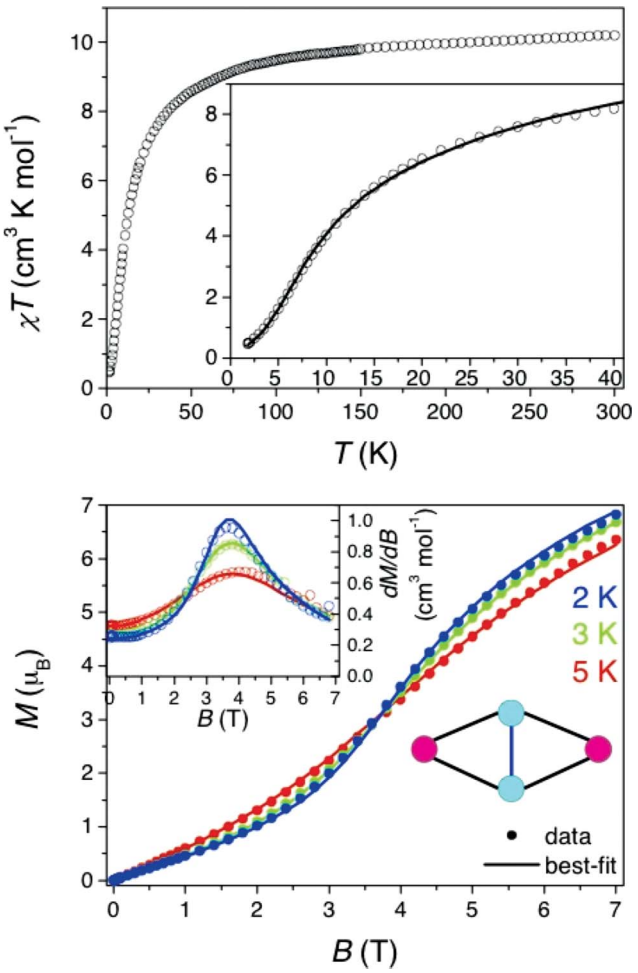

Fig. 5 Plots of χT *vs.* T under applied dc field of 0.1 T (upper) and M *vs.* B curves at the indicated temperatures (lower) for **3**. Circles represent the experimental data. Solid lines are fits with the model discussed in the text. Inset to upper panel: χT *vs.* T in the temperature range used in the fitting. Left inset to lower panel: dM/dB curves as function of applied field. Right inset to lower panel: Sketch of the assumed coupling scheme.

becomes μ_B $\mathbf{s}_i \cdot \mathbf{g}_i \cdot \mathbf{B}$, and the exchange interaction between two Co(II) ions $\mathbf{s}_i \cdot \mathbf{J}_{ij} \cdot \mathbf{s}_j$, where the indices refer to the i-th and j-th Co(II) ion in the cluster, and $\mathbf{g}_i$ matrices and $\mathbf{J}_{ij}$ tensors account for the typically large anisotropy. The coupling tensor $\mathbf{J}_{ij}$ describes both isotropic and anisotropic exchange (antisymmetric exchange is neglected). For compounds **1** and **3**, this results in a spin Hamiltonian, which, however, in general would involve more than hundred magnetic parameters. Hence, the following reasonable assumptions were made.

First, all $\mathbf{g}_i$ matrices and $\mathbf{J}_{ij}$ tensors were assumed to be diagonal and involve a parameter for the xy and one for the z direction, *i.e.*, to be uniaxial. Secondly, the $\mathbf{g}_i$ matrices were assumed to be equal for all ions. Thirdly, not more than two different exchange coupling paths were considered. And finally, the magnetization curves at the different temperatures and the χT data up to 40 K were simultaneously used in the fitting procedure. The Hamiltonian is given in eqn (7), where the first sum should be restricted to those exchange pathways considered in the specific model, which are sketched in Fig. 4 and 5 for compound **1** and **3**, respectively.

$$H = -\sum_{i<j}\left(J_{ij,xy}\mathbf{s}_i \cdot \mathbf{s}_j + \left(J_{ij,z} - J_{ij,xy}\right)\mathrm{s}_{i,z}\mathrm{s}_{j,z}\right) + \mu_B \sum_i \left(g_{xy}\left(\mathrm{s}_{i,x}B_x + \mathrm{s}_{i,y}B_y\right) + \mathrm{g}_z \mathrm{s}_{i,z}B_z\right) \quad (7)$$

For **1** excellent fits to the measured data were obtained for two models. In a first approach, the "one-J" model, all coupling paths were assumed to be equal, *i.e.*, $J_{\mathrm{out},xy} = J_{\mathrm{in},xy} = J_{xy}$ and $J_{\mathrm{out},z} = J_{\mathrm{in},z} = J_z$. The fit converged to a unique parameter set with J_{xy} = –23.0(2) K, J_z = 10.2(1) K, g_{xy} = 3.94(4), and g_z = 6.75(2). In the more realistic "two-J" model, the exchange couplings on the outer hexagon were allowed to differ from the coupling to the central Co(II) ion. A unique parameter set was found with the parameters $J_{\mathrm{out},xy}$ = –23.4(1) K, $J_{\mathrm{out},z}$ = 14.8(2) K, $J_{\mathrm{in},xy}$ = –13.9(6) K, $J_{\mathrm{in},z}$ = 5.2(2) K, g_{xy} = 4.59(2), and g_z = 6.28(2). The resulting fit curves are compared to the experimental data for both models in Fig. 4; the agreement is generally very good.

Compound **3** contains Co(II) ions with both octahedral and trigonal bipyramidal ligand environment. The octahedral Co(II) ions were described as before by effective spins 1/2. For a trigonal bipyramidal Co(II) the orbital angular momentum is quenched and the standard spin Hamiltonian with S_i = 3/2 becomes valid. Thus, the $\mathbf{g}_i$ matrices are almost isotropic with diagonal entries close to 2, the magnetic anisotropy is described by a term $D\,S_{i,z}^2$, and the exchange interactions between the trigonal bipyramidal coordinated Co(II) ions is isotropic. Least-square fits using such models yielded excellent fits but suffered from over-parameterization. However, all good fits yielded a large value for D, leading to well separated ground state doublets. Hence, at low temperatures, also the two trigonal bipyramidal Co(II) ions in **3** can be described by the effective spin-1/2 approach.[19] Again assuming all exchange coupling paths to be equal, a unique fit to the data was obtained, with the parameters J_{xy} = –1.6(1) K, J_z = –38.5(2) K, g_{xy} = 3.87(2), and g_z = 8.10(4). The best-fit curves are shown in Fig. 5. The model excellently reproduces the data, in particular the S-shape and the crossing in the magnetization curves. Fits including two coupling constants were of excellent quality, but highly over-parameterized.

In order to better understand the behaviour of the magnetization curves, simulations were carried out for an assumed single-crystal sample with the external magnetic field applied along and perpendicular to the quantization axis z, Fig. 6. The figure also presents the calculated zero-field energy spectrum, with the levels classified by the magnetic quantum number $M_z = \langle S_z \rangle$. Due to the antiferromagnetic interactions the ground state belongs to $M_z = 0$, however, very closely followed by another $M_z = 0$ level at *ca* 0.3 K (the small splitting between these two states is related to the small coupling J_{xy}).

The first levels with $M_z = \pm 1$ appear at *ca* 19 K, and the $M_z = \pm 2$ levels are at *ca* 77 K. Hence, since the Zeeman splitting will lower the energies of the M_z = –1 and –2 levels with increasing field, level crossings and associated steps in the magnetization curve are observed at $B_{\mathrm{LC},1}$ = 3.45 T and $B_{\mathrm{LC},2}$ = 10.8 T, where the ground state changes from $M_z = 0$ to $M_z = -1$, and $M_z = -1$ to $M_z = -2$. This explains the overall S-shaped M *vs.* B curves and crossing measured in the experiment.

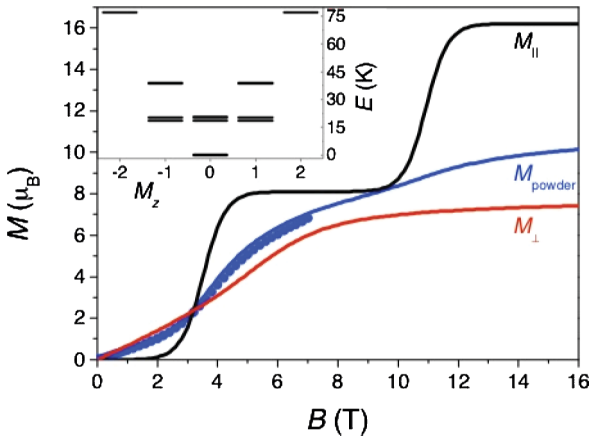

Fig. 6 Plot of M *vs.* B for **3** measured at 2 K (blue dots), and best-fit simulations (blue line). Also shown are the simulated curves for a single-crystal sample with the applied magnetic field parallel (black line) and perpendicular (red line) to the anisotropy (z) axis. The inset shows the calculated zero-field energy spectrum as function of $M_z = \langle S_z \rangle$.

However, the magnetization with the field perpendicular to the z axis displays a very different field dependence, which is due to the large anisotropy ($J_z - J_{xy}$), as compared to the isotropic part ($2J_{xy} + J_z$)/3 of the exchange coupling (which is three times smaller). In fact, in a perpendicular field the Zeeman term does not lead to a splitting of the $M_z = 0$ levels in first order, but to a mixing of levels in second-order. Hence, the energies do vary quadratically with the magnetic field, which gives rise to an essentially linear field dependence of the magnetization, as seen in Fig. 6 at low fields, and not a magnetization step as for fields along z. At larger fields, first-order Zeeman splitting between $M_z \neq 0$ levels comes into play, leading to saturation (at $2\mu_B g_{xy}$).

The physical mechanism discussed above on the quantum level underlies the magnetic behaviour in **3**. However, the large magnetic anisotropy efficiently suppresses quantum fluctuations, leading to a classical picture in terms of spin configurations,[8b] which provides an intuitive understanding of the observed magnetization: in magnetic fields parallel to the anisotropy axis, the initially antiferromagnetically aligned spins are successively flipped one by one such as to overcome the exchange interaction, giving rise to magnetization steps. In contrast, in perpendicular fields, the spins do not flip but slowly tilt towards the magnetic field such as to eventually reach the fully polarized spin configuration. This phenomenon is in fact well known in bulk antiferromagnetic materials as metamagnetism, but is realized here in a single molecule, which is still rare.[8b] This single-molecule metamagnetic behaviour can be contrasted to the slow relaxation behaviour seen in single-molecule magnets (including of Co(II)[8a]) where for SMMs the total spin direction reverses rather than the individual spins undergoing successive flipping. Finally, at this stage in research on the magnetic behaviour of Co(II) molecular systems, it is not yet possible to draw useful conclusions concerning magnetostructural correlations since there are still relatively few examples from which to compile a list of trends coupled with the fact that the nature of the coupling can be ambiguous as a result of the high anisotropy of the metal ion.

Experimental

General Information

All reactions were carried out using standard Schlenk techniques under an inert atmosphere of nitrogen. THF and Et_2O were distilled from sodium-benzophenone. Commercial NaH (60% dispersion in mineral oil), HL (pyridine-2-ylmethanol), and anhydrous $CoCl_2$ were purchased from Aldrich and used as received. Elemental analyses were performed by the microanalytical laboratory in house. The FTIR spectra reported below were collected on a Thermo-Nicolet 67000 spectrometer, equipped with a diamond crystal SMART ORBIT accessory. The FTIR spectra were compared with those recorded on single crystals, collected with a Thermo-Nicolet Centaurus microspectrometer in a microcompression cell with diamond windows.

Preparation of $[Co_7(L)_{12}]Cl_2$ (1), $[Co_6Na(L)_{12}]Cl$ (2) and $[Co_4(L)_6Cl_2]$ (3)

(a) To a Schlenk tube containing a stirred slurry of anhydrous $CoCl_2$ (0.300 g, 2.31 mmol) in THF (100 mL) were added liquid pyridine-2-ylmethanol (0.453 g, 4.16 mmol) and NaH (60% suspension in mineral oil, 0.231 g, 5.78 mmol). Evolution of H_2 was observed and the Schlenk tube was purged with an argon flow, until the evolution of gas ceased. The suspension was stirred for 12 h and the solution was filtered (A). The solid residue was extracted with CH_2Cl_2 (70 mL, B) and this solution B was filtered and layered with Et_2O (100 mL). A mixture of dark orange crystals of **1** and violet crystals of **3** was obtained. The mother liquor was removed but the crystals were not dried. Instead, 20 mL of dichloromethane were added until dissolution of **1** was complete (solution C), whereas the crystals of **3** dissolved much more slowly and could therefore more easily be collected. Applying twice this procedure on the CH_2Cl_2 solution C, afforded spectroscopically pure samples of **1** and **3** (yields: 0.223 g, 38%, based on cobalt for **1**; 0.193 g, 35% for **3**). Drying the crystals of **1** and **3** under reduced pressure resulted in loss of crystallinity. The THF solution A (see above) was layered with Et_2O and gave, in low yields, red crystals of **2** (Yield: 0.033 mg, 5%, based on Co).

(b) To a Schlenk tube containing a stirred slurry of anhydrous $CoCl_2$ (0.300 g, 2.31 mmol) in THF (100 mL), liquid pyridine-2-ylmethanol (0.556 g, 5.10 mmol) and NaH (60% suspension in mineral oil, 0.278 g, 6.96 mmol) were added. Evolution of H_2 was observed and the Schlenk tube was purged with an argon flow, until the evolution of gas ceased. The suspension was stirred for 12 h and the solution was filtered. The orange solid residue was washed with THF (40 mL), extracted with CH_2Cl_2 (30 mL). This solution was filtered and the filtrate layered with Et_2O (20 mL) and pentane (60 mL). Dark orange crystals of **1** were obtained (yield: 0.330 g, 56%, based on cobalt).

(c) To a Schlenk tube containing a freshly prepared suspension of anhydrous $CoCl_2$ (0.300 g, 2.31 mmol) in THF (100 mL), liquid pyridine-2-ylmethanol (0.405 g, 3.71 mmol) was quickly added. Solid NaH (60% suspension in mineral oil, 0.186 g, 4.64 mmol) was added to this suspension. Evolution of H_2 was observed and the Schlenk tube was purged with an argon flow, until the evolution of gas ceased. The violet suspension was stirred for 2 h and the solution was filtered *via* a cannula. The residue was washed twice with THF (70 mL). The solid residue was extracted with CH_2Cl_2

(2×50 mL) and this solution was filtered and layered with Et_2O (40 mL). Dark violet crystals of **3** were obtained (yield: 0.320 g, 58% based on cobalt).

(d) To a solution of HL (0.250 g, 2.30 mmol) in THF (40 mL), NaH was added (60% in mineral oil, 0.120 g, 3.00 mmol). Evolution of H_2 was observed and the Schlenk tube was purged with an argon flow, until the evolution of gas ceased. To this suspension, a suspension of $CoCl_2$ (0.130 g, 1.00 mmol) in THF (40 mL) was added. The colour of the suspension became immediately pale orange. Stirring was continued for 2 h and the suspension was collected by filtered. Dichloromethane was added (30 mL) to this solid residue and the resulting suspension was stirred for 30 min and filtered. The filtrate was layered with dry THF as interlayer (3 mL), then with Et_2O (20 mL) and finally with hexane (50 mL). Orange crystals of **1** were obtained after few days (yield: 0.140 g, 54% based on cobalt).

Anal. Calcd. for $C_{72}H_{72}Cl_2Co_7N_{12}O_{12}$ (**1**, M = 1780.85): (%): C, 48.56; H, 4.07; N, 9.43. Found, after drying: C, 48.44; H, 4.44; N, 9.34; for $C_{72}H_{72}ClCo_6N_{12}NaO_{12}$ (**2**, M = 1768.39): (%): C, 50.59; H, 4.25; N, 9.83. Found, after drying: C, 50.48; H, 4.53; N, 9.63; for $C_{36}H_{36}Cl_2Co_4N_6O_6$ (**3**, M = 955.35): (%): C, 45.26; H, 3.80; N, 8.80. Found, after drying: C, 45.41; H, 3.56; N, 9.13. FTIR spectra of compounds **1**, **2** and **3** are reported in the ESI.†

Conversion of $[Co_4(L)_6Cl_2]$ (3) to $[Co_7(L)_{12}]Cl_2$ (1)

To a Schlenk tube containing a stirred slurry of **3** (0.340 g, 0.36 mmol) in THF (80 mL), NaH (60% suspension in mineral oil, 0.022 g, 0.54 mmol) was added. Liquid pyridine-2-ylmethanol (0.039 g, 0.36 mmol) was added and the suspension was stirred for 4 h. The solid was collected by filtration, washed with THF (40 mL) and extracted with CH_2Cl_2 (60 mL). Hexane (100 mL) was layered onto the filtrate and orange crystals of cluster **1** were collected by filtration and dried under vacuum (Yield: 0.152 g, 42%).

Conversion of $[Co_7(L)_{12}]Cl_2$ (1) to $[Co_4(L)_6Cl_2]$ (3)

To a Schlenk tube containing a solution of **1** (0.280 g, 0.16 mmol) in CH_2Cl_2 (50 mL), anhydrous $CoCl_2$ was added (0.024 g, 0.18 mmol). The suspension was sonicated for 20 min and stirred for 2 h. The resulting violet solution was filtered and the filtrate precipitated with pentane (100 mL), giving **1** as a pale violet powder (Yield, based on **1**: 0.270 g, 90%).

Conversion of $[Co_7(L)_{12}]Cl_2$ (1) to $[Co_4(L)_4Cl_4(MeOH)_4]$

To a Schlenk tube containing a solution of **1** (0.340 g, 0.19 mmol) in CH_2Cl_2 (60 mL), anhydrous $CoCl_2$ was added (0.100 g, 0.77 mmol). After 30 min the solution colour turned violet and formation of cluster **1** was observed spectroscopically by sampling an aliquot of the suspension, centrifugating and precipitating with pentane. The solid sample was analyzed by FTIR spectroscopy (see ESI). After stirring for 1 h, the suspension was filtered, and pentane (100 mL) was added to the filtrate, resulting in the precipitation of a greyish powder, which was analyzed by FTIR (see ESI†). This solid was then dissolved in methanol and the resulting solution was left evaporating. Purple crystals of $[Co_4(L)_4Cl_4(MeOH)_4]$ formed quickly.

Observation of $[Co_6Mg(L_{12})]^{2+}$ and $[CaCo_6(L_{12})]^{2+}$

Freshly prepared NaL powder (0.150 g, 1.15 mmol), anhydrous $CoCl_2$ (0.060 g, 0.46 mmol) and anhydrous MCl_2 (7.3 mg for M = Mg, 8.9 mg for M = Ca, 0.08 mmol) were weighted into a 20 mL test tube inside a glovebox. Dry THF (8 mL) was added and the mixture was stirred for 12 h. The reaction mixture was filtered and the yellow solid residue was collected and then dissolved in 3 mL of dry CH_2Cl_2. This solution was filtered and subjected for ESI-MS test under high flow mode at 150 °C. Mass spectra are shown in the ESI† to this paper.

Magnetic measurements

Magnetic susceptibility data (1.8–300 K) were collected on powdered samples using a Quantum Design MPMS-XL SQUID magnetometer under a 1000 Oe applied magnetic field. Magnetization isotherms were collected between 0 and 7 T at 2, 3 and 5 K. All data were corrected for the contribution of the sample holder.

X-ray data collection, structure solution and refinement for 1, 2 and 3

Suitable crystals for the X-ray analysis of **1**, **2** and **3** were obtained as described below. The intensity data were collected at 173(2) K on a Kappa CCD diffractometer[20] (graphite monochromated Mo-Kα radiation, λ = 0.71073 Å). The structures were solved by direct methods (SHELXS-97) and refined by full-matrix least-squares procedures (based on F^2, SHELXL-97)[21] with anisotropic thermal parameters for all the non-hydrogen atoms. The hydrogen atoms were introduced into the geometrically calculated positions (SHELXS-97 procedures) and refined *riding* on the corresponding parent atoms. Details on the refinement of the structures can be found in the ESI. CCDC 821779–821781 contain the supplementary crystallographic data for this paper that can be obtained free of charge from the Cambridge Crystallographic Data Center *via* www.ccdc.cam.ac.uk/data_request/cif.

Conclusions

By careful investigation of the reactions between pyridine-2-ylmethanol (HL), anhydrous $CoCl_2$ and NaH in various proportions and as a function of the solvent, we have been able to isolate various polynuclear Co(II) complexes $[Co_7(L)_{12}]Cl_2$ (**1**), $[Co_6Na(L)_{12}]Cl$ (**2**) and $[Co_4Cl_2(L)_6]$ (**3**). Whereas X-ray diffraction established that **1** and **2** possess a $M@M_6$ Anderson-type structure with six face-sharing incomplete cubane moieties arranged in a cyclic manner leading to a planar arrangement of the metal centres, the structure of **3** is that of a defective double cubane, with a missing apex in each sub-structure. This results in the assembling of two six coordinate Co(II) centres in a distorted octahedral coordination geometry with two five coordinate Co(II) centres in a trigonal bipyramidal coordination environment. Magnetic studies indicated an overall antiferromagnetic coupling between the paramagnetic Co(II) ions of **1** whereas the behaviour of **3** corresponds to a situation where the magnetic field overcomes the antiferromagnetic interactions allowing for the parallel alignment of the spins, which, however, owing to the strong magnetic anisotropy in the Co(II) cluster is of the metamagnetic type. The experimental conditions set for the synthesis of these complexes,

in particular the HL : $CoCl_2$ ratio, play a critical role and this has allowed us to determine the optimum conditions for the isolation of a given complex. Furthermore, we have established that in the presence of added ligand or $CoCl_2$, an interconversion between these complexes is possible. Such studies provide a more rational synthesis of polynuclear Co(II) complexes, which is highly desirable if one wishes to establish structure/properties relationships. There is little doubt that more complexes remain to be discovered with such types of N,O-ligands.

Acknowledgements

We thank Melanie Boucher (LCC, Strasbourg) and Wang Pei (Singapore) for experimental assistance, Laure Kayser (Master student LCC Strasbourg and currently PhD student at McGill University, Montreal) for discussions. We thank the CNRS, the Ministère de l'Enseignement Supérieur et de la Recherche (Paris), the Université de Strasbourg, the **I**nternational **C**enter for **F**rontier **R**esearch in **C**hemistry, Strasbourg (icFRC, www.icfrc.fr), the French Embassy in Singapore, the Agency for Science, Technology & Research (Singapore) and the National University of Singapore (NUS) (R143-000-277-305) for support. Y. Lan and A. K. Powell (KIT, Germany) would like to acknowledge support from the DFG Center for Functional Nanostructures.

Notes and references

1 (*a*) S. Parsons and R. E. P. Winpenny, *Acc. Chem. Res.*, 1997, **30**, 89–95; (*b*) R. E. P. Winpenny, *J. Chem. Soc., Dalton Trans.*, 2002, 1–10; (*c*) S. Langley, M. Helliwell, J. Raftery, E. I. Tolis and R. E. P. Winpenny, *Chem. Commun.*, 2004, 142–143; (*d*) S. J. Langley, M. Helliwell, R. Sessoli, P. Rosa, W. Wernsdorfer and R. E. P. Winpenny, *Chem. Commun.*, 2005, 5029–5031; (*e*) S. Langley, M. Helliwell, R. Sessoli, S. J. Teat and R. E. P. Winpenny, *Inorg. Chem.*, 2008, **47**, 497–507; (*f*) S. Langley, M. Helliwell, R. Sessoli, S. J. Teat and R. E. P. Winpenny, *Dalton Trans.*, 2009, 3102–3110.

2 T. Taguchi, W. Wernsdorfer, K. A. Abboud and G. Christou, *Inorg. Chem.*, 2010, **49**, 10579–10589; M. Morimoto, H. Miyasaka, M. Yamashita and M. Irie, *J. Am. Chem. Soc.*, 2009, **131**, 9823–9835; J. Lawrence, E. C. Yang, D. N. Hendrickson and S. Hill, *Phys. Chem. Chem. Phys.*, 2009, **11**, 6743–6749; C. G. Efthymiou, C. Papatriantafyllopoulou, N. I. Alexopoulou, C. P. Raptopoulou, R. Boca, J. Mrozinski, E. G. Bakalbassis and S. P. Perlepes, *Polyhedron*, 2009, **28**, 3373–3381; E. Ruiz, T. Cauchy, J. Cano, R. Costa, J. Tercero and S. Alvarez, *J. Am. Chem. Soc.*, 2008, **130**, 7420–7426; J. Lawrence, E.-C. Yang, R. Edwards, M. M. Olmstead, C. Ramsey, N. S. Dalal, P. K. Gantzel, S. Hill and D. N. Hendrickson, *Inorg. Chem.*, 2008, **47**, 1965–1974; E.-C. Yang, W. Wernsdorfer, L. N. Zakharov, Y. Karaki, A. Yamaguchi, R. M. Isidro, G.-D. Lu, S. A. Wilson, A. L. Rheingold, H. Ishimoto and D. N. Hendrickson, *Inorg. Chem.*, 2006, **45**, 529–546; E.-C. Yang, W. Wernsdorfer, S. Hill, R. S. Edwards, M. Nakano, S. Maccagnano, L. N. Zakharov, A. L. Rheingold, G. Christou and D. N. Hendrickson, *Polyhedron*, 2003, **22**, 1727–1733.

3 (*a*) L. Kayser, R. Pattacini, G. Rogez and P. Braunstein, *Chem. Commun.*, 2010, **46**, 6461–6463; (*b*) J. Zhang, P. Teo, R. Pattacini, A. Kermagoret, R. Welter, G. Rogez, T. S. A. Hor and P. Braunstein, *Angew. Chem., Int. Ed.*, 2010, **49**, 4443–4446.

4 T. Baruah and M. R. Pederson, *Chem. Phys. Lett.*, 2002, **360**, 144–148; E.-C. Yang, D. N. Hendrickson, W. Wernsdorfer, M. Nakano, L. N. Zakharov, R. D. Sommer, A. L. Rheingold, M. Ledezma-Gairaud and G. Christou, *J. Appl. Phys.*, 2002, **91**, 7382–7384; T. Baruah and M. R. Pederson, *Int. J. Quantum Chem.*, 2003, **93**, 324–331; J. Liu, S. Datta, E. Bolin, J. Lawrence, C. C. Beedle, E.-C. Yang, P. Goy, D. N. Hendrickson and S. Hill, *Polyhedron*, 2009, **28**, 1922–1926.

5 For a recent example of another cubane-like SMM see *e.g.*: Scheurer, A. M. Ako, R. W. Saalfrank, F. W. Heinemann, F. Hampel, K. Petukhov, K. Gieb, M. Stocker and P. Müller, *Chem.–Eur. J.*, 2010, **16**, 4784–4792.

6 M. Murrie, *Chem. Soc. Rev.*, 2010, **39**, 1986–1995 and references therein.

7 (*a*) F. E. Mabbs and D. J. Machin, *Magnetism and Transition Metal Complexes*, Chapman and Hall, London, 1973; (*b*) F. Lloret, M. Julve, J. Cano, R. Ruiz-García and E. Pardo, *Inorg. Chim. Acta*, 2008, **361**, 3432–3445.

8 (*a*) F. Klöwer, Y. Lan, J. Nehrkorn, O. Waldmann, C. E. Anson and A. K. Powell, *Chem.–Eur. J.*, 2009, **15**, 7413; (*b*) O. Waldmann, M. Ruben, U. Ziener, P. Müller and J. M. Lehn, *Inorg. Chem.*, 2006, **45**, 6535.

9 R. D. Shannon, *Acta Cryst.*, 1976, **A32**, 751–76.

10 K. G. Alley, R. Bircher, O. Waldmann, S. T. Ochsenbein, H. U. Güdel, B. Moubaraki, K. S. Murray, F. Fernandez-Alonso, B. F. Abrahams and C. Boskovic, *Inorg. Chem.*, 2006, **45**, 8950–8957; M. Moragues-Canovas, C. E. Talbot-Eeckelaers, L. Catala, F. Lloret, W. Wernsdorfer, E. K. Brechin and T. Mallah, *Inorg. Chem.*, 2006, **45**, 7038–7040; A. Ferguson, A. Parkin, J. Sanchez-Benitez, K. Kamenev, W. Wernsdorfer and M. Murrie, *Chem. Commun.*, 2007, 3473–3475; L. F. Chibotaru, L. Ungur, C. Aronica, H. Elmoll, G. Pilet and D. Luneau, *J. Am. Chem. Soc.*, 2008, **130**, 12445–12455; V. Tudor, G. Marin, F. Lloret, V. C. Kravtsov, Y. A. Simonov, M. Julve and M. Andruh, *Inorg. Chim. Acta*, 2008, **361**, 3446–3452.

11 Y.-L. Zhou, M.-H. Zeng, L.-Q. Wei, B.-W. Li and M. Kurmoo, *Chem. Mater.*, 2010, **22**, 4295–4303.

12 Y.-Z. Zhang, W. Wernsdorfer, F. Pan, Z.-M. Wang and S. Gao, *Chem. Commun.*, 2006, 3302–3304; X.-T. Wang, B.-W. Wang, Z.-M. Wang, W. Zhang and S. Gao, *Inorg. Chim. Acta*, 2008, **361**, 3895–3902.

13 B. Cordero, V. Gómez, V. A. E. Platero-Prats, M. Revés, J. Echeverría, E. Cremades, F. Barragán and S. Alvarez, *Dalton Trans.*, 2008, 2832–2838.

14 For recent examples of oxygen-bridged Na@Tr6 structures (Tr = transition metal) see, *e.g.*: Y. Li, Q. Wu, L. Lecren and R. Clérac, *J. Mol. Struct.*, 2008, **890**, 339–345; P.-P. Yang, H.-B. Song, X.-F. Gao, L.-C. Li and D.-Z. Liao, *Cryst. Growth Des.*, 2009, **9**, 4064–4069.

15 For recent examples see, *e.g.*: A. Ferguson, A. Parkin and M. Murrie, *Dalton Trans.*, 2006, 3627–3628; Z. Chen, Y. Li, C. Jiang, F. Liang and Y. Song, *Dalton Trans.*, 2009, 5290–5299; S.-H. Zhang, Y. Song, H. Liang and M.-H. Zeng, *CrystEngComm*, 2009, **11**, 865–872.

16 G. A. Seisenbaeva, M. Kritikos and V. G. Kessler, *Polyhedron*, 2003, **22**, 2581–2586.

17 S. G. Telfer, R. Kuroda, J. Lefebvre and D. B. Leznoff, *Inorg. Chem.*, 2006, **45**, 4592–4601.

18 P. Sobota, Z. Olejnik, J. Utko and T. Lis, *Polyhedron*, 1993, **12**, 613–616.

19 (*a*) A. Abragam and B. Bleaney, *Electron Paramagnetic Resonance of Transition Ions*Clarendon Press, Oxford, 1970; (*b*) A. Abragam and M. H. L. Pryce, *Proc. R. Soc. London Ser. A*, 1950, **206**, 173.

20 Bruker-Nonius, *Kappa CCD Reference Manual*, Nonius BV, The Netherlands, 1998.

21 G. M. Sheldrick, *Acta Cryst.*, 2008, **A64**, 112.

